Acta of Bioengineering and Biomechanics
Vol. 23, No. 2, 2021

Original paper
DOI: 10.37190/ABB-01782-2021-05

Thermally stable biopolymer composites based on poly(3-hydroxybutyrate) modified with linear aliphatic polyurethanes – preparation and properties

IWONA ZARZYKA[1]*, ANNA CZERNIECKA-KUBICKA[2, 3], KAROL HĘCLIK[1], LUCJAN DOBROWOLSKI[1], MAREK PYDA[1], KAROLINA LEŚ[1], MAŁGORZATA WALCZAK[1], ANITA BIAŁKOWSKA[4], MOHAMED BAKAR[4]

[1] Faculty of Chemistry, Rzeszów University of Technology, Rzeszów, Poland.
[2] Department of Experimental and Clinical Pharmacology, Medical College of Rzeszów University, The University of Rzeszów, Rzeszów, Poland.
[3] Faculty of Mechanics and Technology, Rzeszow University of Technology, Stalowa Wola, Poland.
[4] Faculty of Chemical Engineering and Commodity Science, University of Technology and Humanities, Radom, Poland.

Purpose: Poly(3-hydroxybutyrate) (P3HB) is a biopolymer, but storing products from P3HB causes the deterioration of their properties leading to their brittleness. P3HB has also low thermal stability. Its melting point almost equals its degradation temperature. To obtain biodegradable and biocompatible materials characterized by higher thermal stability and better strength parameters than the unfilled P3HB, composites with the addition of polyurethanes were produced. *Methods*: The morphology, thermal, and mechanical property parameters of the biocomposites were examined using scanning electron microscopy, thermogravimetric analysis, standard differential scanning calorimetry, and typical strength machines. *Results*: Aliphatic polyurethanes, obtained by the reaction of 1,6-hexamethylene diisocyanate and polyethylene glycols, were used as modifiers. To check the influence of the glycol molar mass on the properties of the biocomposites, glycols with a molecular weight of 400 and 1000 g/mol were used. New biocomposites based on P3HB were produced with 5, 10, 15, and 20 wt. % content of polyurethane by direct mixing using a twin-screw extruder. The following property parameters of the prepared biocomposites were tested: degradation temperature, glass transition temperature, tensile strength, impact strength, and Brinell hardness. *Conclusions*: Improvement of the processing property parameters of P3HB-biocomposites with the addition of aliphatic polyurethanes was achieved by increasing the degradation temperature in relation to the degradation temperature of the unfilled P3HB by over 30 °C. The performance property parameters have also been improved by reducing the brittleness compared to the P3HB, as evidenced by the increase in impact strength and the decrease in hardness with an increase in the amount of polyurethane obtained by the reaction of 1,6-hexamethylene diisocyanate and polyethylene glycol with a molecular weight of 400 g/mol (PU400) as modifier.

Key words: *biocomposites, poly(3-hydroxybutyrate), linear aliphatic polyurethanes, thermal stability, degradation temperature, mechanical property parameters*

1. Introduction

Poly(3-hydroxybutyrate) (P3HB) is a biosynthesized, biodegradable and biocompatible polyhydroxyalkanoate used in combination or alone for biomedical applications, such as: sutures, repair devices and patches, cardiovascular patches, orthopedic pins, adhesion barriers, stents, guided tissue repair/regeneration devices, articular cartilage repair devices, nerve guides, tendon repair devices, bone marrow scaffolds, and wound dressings [1], [8], [17], [18]. Unfortunately, P3HB products are

* Corresponding author: Iwona Zarzyka, Faculty of Chemistry, Rzeszów University of Technology, ul. Powstańców Warszawy 6, 35-959, Rzeszów, Poland, e-mail: izarzyka@prz.edu.pl, tel.: +480178651762, fax.: +480178543655
Received: January 4th, 2021
Accepted for publication: March 31st, 2021

brittle and stiff and characterized by low thermostability. Its decomposition temperature is slightly higher than its melting point, therefore its use in the production of biodegradable products is limited [15], [16].

To improve the property parameters s of P3HB, its copolymers are synthesized with other aliphatic hydroxy acids, e.g., 4-hydroxybutyric acid, 3-hydroxyvaleric acid or 3-hydroxyhexanoic acid. P3HB terpolymers with the use of 3-hydroxypropionic acid, and lactic acid or involving 4-hydroxybutyric acid and lactic acid or P3HB quaterpolymers with the use of 4-hydroxybutyric acid, 3-hydroxypropionic acid and lactic acid are also produced [2], [6], [19], [20], [24].

The thermal stability of P3HB can also be improved by grafting maleic anhydride onto it. The purified grafted P3HB has a higher degradation temperature, increased by at least 50 °C and better thermal stability than the unmodified P3HB. Moreover, it does not tend to decrease in a molecular weight during a heat treatment. At the same time, the crystallization rate, melting point, and crystallinity of P3HB are increased [10].

There is also a known method of improving the property parameters of P3HB by preparing its blend with other polymers having the desired property parameters or by adding an appropriate plasticizer [3].

The polymer blends of P3HB and polylactic acid are characterized by better mechanical property parameters than the unmodified P3HB in retaining its biodegradability [9]. Similarly, the blend of poly(3-hydroxybutyrate-*co*-3-hydroxyvalerate) copolymer with poly(butylene adipate)terephthalate and epoxy-terminated hyperbranched polyester has also enhanced mechanical property parameters [23].

There are also known methods of improving the thermal and mechanical property parameters of P3HB by producing its polymer composites or using its polymer blends or its copolymer as a matrix. Materials with better property parameters, usually impossible to obtain in any other way, are obtained by combining the polymer matrix with the filler.

The P3HB-based composites with glass fiber and talc show excellent thermal stability, resistance to hydrolysis, good mechanical strength, and easy formability [22]. P3HB composites with the addition of carbodiimide compounds and talc show reduced flammability, good thermal stability, resistance to moisture, and good mechanical strength [14]. Composites made on the basis of P3HB polymer blend and acrylate-methacrylate block copolymer containing talc as a filler show improved mechanical and thermal property parameters compared to the unmodified P3HB [12]. The composites based on the polymer blend of P3HB and aromatic polycarbonate with talc and glass fiber as fillers characterized by the excellent thermal stability and impact strength [13].

The aim of the present work was to produce new poly(3-hydroxybutyrate) biocomposites with a polyurethane modifier (5–20 wt. %), which are characterized by better thermal property parameters, processing parameters, and better mechanical property parameters than the unmodified P3HB. Aliphatic linear polyurethane was obtained by reacting of 1,6-hexamethylene diisocyanate and polyethylene glycol with a molecular weight of 400 g · mole^{-1} or 1000 g · mole^{-1}.

Considering the biocompatibility of polyurethanes and P3HB [7], [11], the produced biocomposites are promising candidates for the production of medical materials.

2. Materials and methods

2.1. Materials

P3HB was supplied by Biomer (Krailling, Germany). Weight average molecular mass of P3HB is M_w = 443,900 g · mol^{-1} and its dispersity $M_w \cdot M_n^{-1}$ = 5.72 [–] measured by the size exclusion chromatography in chloroform. P3HB melt flow index is 0.11 g · (10 min)$^{-1}$ (180 °C at 2.16 kg). Hexamethylene 1,6-diisocyanate (HDI) and dibutyltin(IV) dilaurate (DBTL) were supplied by Sigma-Aldrich (Saint Louis, Missouri, US) and polyethylene glycols by Merck (Darmstadt, Germany). Acetone (high purity) was supplied by Chemsolute (Munich, Germany).

2.2. Polyurethane preparation

First, polyols were purified by means of azeotropic distillation with toluene to eliminate water. Next, 0.25 mole of polyethylene glycol with a molar mass of 400 g· mole^{-1} (PEG400), 50 cm^3 of dried acetone, and 0.2 cm^3 of DBTL were placed in a flask. The HDI was added dropwise to the solution in such amount that the molar ratio of isocyanate to hydroxyl groups of the glycol was 1:1.08. The dropping rate was controlled to keep the temperature of the reaction mixture below 20 °C. The reaction was carried out under a nitrogen atmosphere. Reaction was completed when the exotherm effect disappeared, on the basis of the increase in the viscosity of the reaction mixture and determination of the isocya-

nate number according to PN-EN 1242.2006. Totally, it lasted up to 6 hours. The polyurethane solution was poured into a large surface vessel and acetone was removed. To give a constant weight of the final product, polyurethane (PU400) was placed in a vacuum oven at 40–100 °C. In a similar way, polyurethane (PU1000) based on polyethylene glycol with a molar mass of 1000 g · mole^{-1} (PEG1000) was prepared. The only difference was the use of double amount of catalyst for synthesis.

2.3. Biocomposites preparation

Biocomposites were obtained by mixing the melt P3HB with 5, 10, 15, and 20 wt. % of polyurethane, PU400, and PU1000 (sample designation is shown in Table 1) in a co-rotating twin screw extruder ZE-25-33D by Berstorff. Previously, P3HB was dried at 40 °C under reduced pressure for 30 min. To obtain a homogeneous mixture of components, P3HB was introduced into a Stephan mixer and the appropriate amount of additive (PU400 or PU1000) was dosed with constant stirring. Earlier PU400 was dissolved in acetone at room temperature and the solution was dosed to P3HB (placed earlier) in mixer. Polyurethane PU1000 was mixed with P3HB in the powder form.

The ingredients were mixed for approx. 20 minutes at room temperature. The homogeneous two-component mixture was put on the extruder. The unfilled P3HB was also extruded as the reference material. The twin screw-extruder was equipped with ten temperature-controlled zones, which were programmed in the range of 20–170 °C. The screw diameter (D) of the extruder was 25 mm and the L · D^{-1} ratio was 33. The screw speed during extrusion was in the range of 300–320 rpm. Extrusion conditions were determined experimentally.

Table 1. Designation of prepared biocomposites

Glycol type in PU	Concentration of PU in biocomposite (wt. %)	Biocomposite designation
PEG400	5	PEG-400/5
PEG400	10	PEG-400/10
PEG400	15	PEG-400/15
PEG400	20	PEG-400/20
PEG1000	5	PEG-1000/5
PEG1000	10	PEG-1000/10
PEG1000	15	PEG-1000/15
PEG1000	20	PEG-1000/20

2.4. Analytical methods

2.4.1. Size exclusion chromatography

Size Exclusion Chromatogrphy (SEC) measurements of the polyurethanes were performed using the following apparatus and measurement conditions: Viscotek degasser, columns (PSS SDV Guard and PSS SDV 100 Å, 1000 Å, grain diameter 5 μm), Shimadzu LC-20AD isocratic pump, Shodex RI-71 differential refractometer, solvent: tetrahydrofuran (THF), sample concentration: 3 mg· ml^{-1}, THF flow rate: 1 ml · min^{-1}, temperature: 22 °C, loop volume: 100 μl, OmniSEC software version 4.2. Number-average ($\overline{M}_n$) and weight-average ($\overline{M}_w$) molar masses and dispersity index (DI = $M_w \cdot M_n^{-1}$) of PU400 and PU1000 were determined and given in Table 2.

Table 2. Molar mass and molar mass distributions of linear PU400 and PU1000

PU	M_n [g·mole^{-1}]	M_w [g·mole^{-1}]	DI = $M_w \cdot M_n^{-1}$ [–]
PU400	5.962	13.433	2.090
PU1000	11.882	16.581	1.395

2.4.2. FTIR spectroscopy

IR spectra of polyurethanes, the extruded P3HB, and the resulting composites were performed using a PARAGON 1000 FTIR apparatus and recorded from 400 cm^{-1} to 4000 cm^{-1}. Spectra were made with the resolution of the order of 0.01 cm^{-1}. Samples were measured by ATR technique. It was taken 128 scans.

2.4.3. Scanning electron microscopy

The morphology tests of the obtained biocomposites were carried out using a JEOL scanning electron microscope, JSM-6490 LV with an X-ray energy dispersion analyzer for chemical analysis in the microarea. The fracture surfaces of the biocomposites samples were tested. For this purpose, the samples were frozen in liquid nitrogen and then they were broken with a hammer. The samples obtained after breaking were covered with a gold layer with a thickness of about 10 nm using a JEOL JFC-1300 gold sputtering machine.

2.4.4. TGA analysis

Thermogravimetric analysis (TGA) was performed using a Metler Toledo TGA/SDTA 851e thermogravimetric analyzer. The samples were heated at a heating rate of 10 °C· min^{-1} or 5 °C· min^{-1} in the temperature range of 25–600 °C in an inert gas (nitrogen) atmosphere. The temperature of decomposition onset (T_{on}), the temperature of 50% mass loss ($T_{50\%}$), the temperature of the maximum decomposition rate (T_{max}), and the total mass loss of the sample at 600 °C were determined.

2.4.5. DSC analysis

Dependences of heat flow rate on temperature were obtained using the differential scanning calorimeter (DSC), Q1000 from TA Instruments. All analyses were carried out in a nitrogen atmosphere with a constant flow rate of around 50 ml·min^{-1}. To obtain very accurate measurements, the temperature calibration and the heat flow rate calibration were performed in reference to the melting parameters of indium, i.e., the onset temperature equals 429.6 K and the heat of fusion, ΔH_f = 28.45 J/g (3.28 kJ/mol) [5], [21]. The calibration of heat capacity was also carried out to improve the quality of the obtained results. Three measurements, i.e., a calibration on sapphire, blank (reference), and actual sample composites were performed for each one of the measured samples. The experiments were performed in the temperature range of –40 °C to 195 °C for heating and next in the temperature range from 195 °C to –40 °C. The data were collected from second heating scan. The measurements were carried out using a different cooling rate in the range of 1 °C·min^{-1} to 40 °C·min^{-1} and the same heating rate of 10 °C·min^{-1}.

2.4.6. Mechanical tests

Samples for mechanical tests were obtained by the injection method using an Arburg 420 M Allrounder 1000-250 injection molding machine equipped with a Priamus production supervision and monitoring system. The samples were made in accordance with the standard PN EN ISO 527 (1998). The process was carried out at the temperature range of 140–168 °C, the temperature of the injection mold was 25 °C for P3HB and 30 °C for the composition. The following mechanical tests were made: tensile strength, impact strength, and Brinell hardness.

Tensile strength

The tensile mechanical property parameters were determined in accordance with PN-EN ISO 527–2:2012 using the Instron 4505 testing machine. Tensile strength and strain at break measurements were carried out under the condition of a deformation rate of 5 mm · min^{-1}.

Impact strength

Charpy notch impact tests were carried out in accordance with PN-EN ISO 179-1:2010 using the Zwick 5102 hammer on sample and a notch length of 1 mm.

Brinell hardness

Hardness was determined by the Brinell method in accordance with the PN-EN ISO 6506-1:2014 standard using the Zwick apparatus.

3. Results

To improve the property parameters of P3HB, composites were produced based on P3HB matrix with aliphatic polyurethanes, based on HDI and polyethylene glycols PEG400 and PEG1000 as a modifier. The unfilled P3HB was also extruded under the same conditions.

The degree of polymerization of polyurethanes was evaluated and the results of SEC measurements were given in Table 2. PU400 had smaller molar masses (M_w = 13,433 g·mole^{-1}) and higher molar mass dispersity of about 2.090 [–] than PU1000 (M_w = 16,581 g·mole^{-1} and ($M_w \cdot M_n^{-1}$ = 1.395 [–]).

3.1. Morphology analysis

SEM was used to explain the possible modifications that may occur in the structure of polymeric systems and consequently explain the changes in their physical property parameters. The surface of unmodified P3HB has a slightly wave-like morphology with few edge lines, as we can see in Fig. 1.

In Figure 2, the SEM micrographs of fracture surfaces of P3HB-based composite samples containing different amounts (5, 10, 15, and 20 wt. %) of PU400 are shwo. The samples contain the polyurethane modifier characterized by the presence of elongated wave-like and rough structures. The higher the amount of polyurethane modifier, the wavier and more irregular

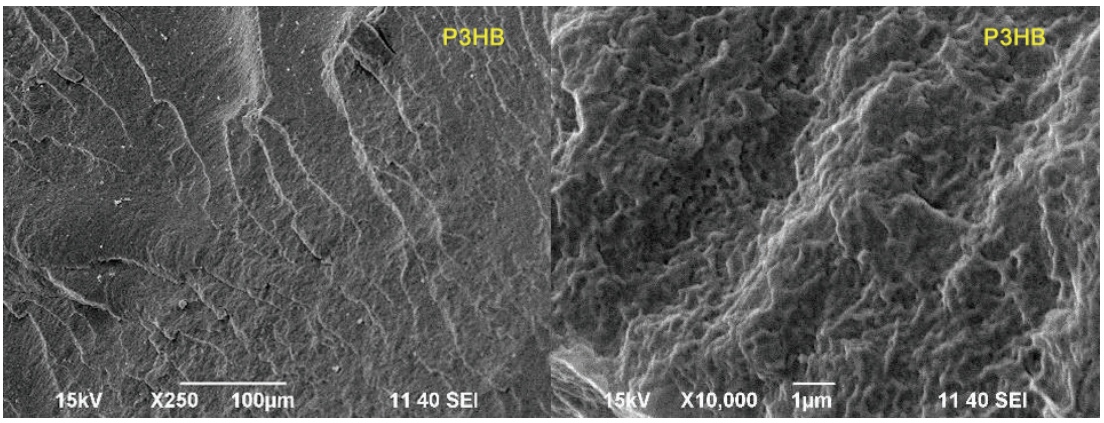

Fig. 1. SEM micrographs of unmodified P3HB with different magnifications

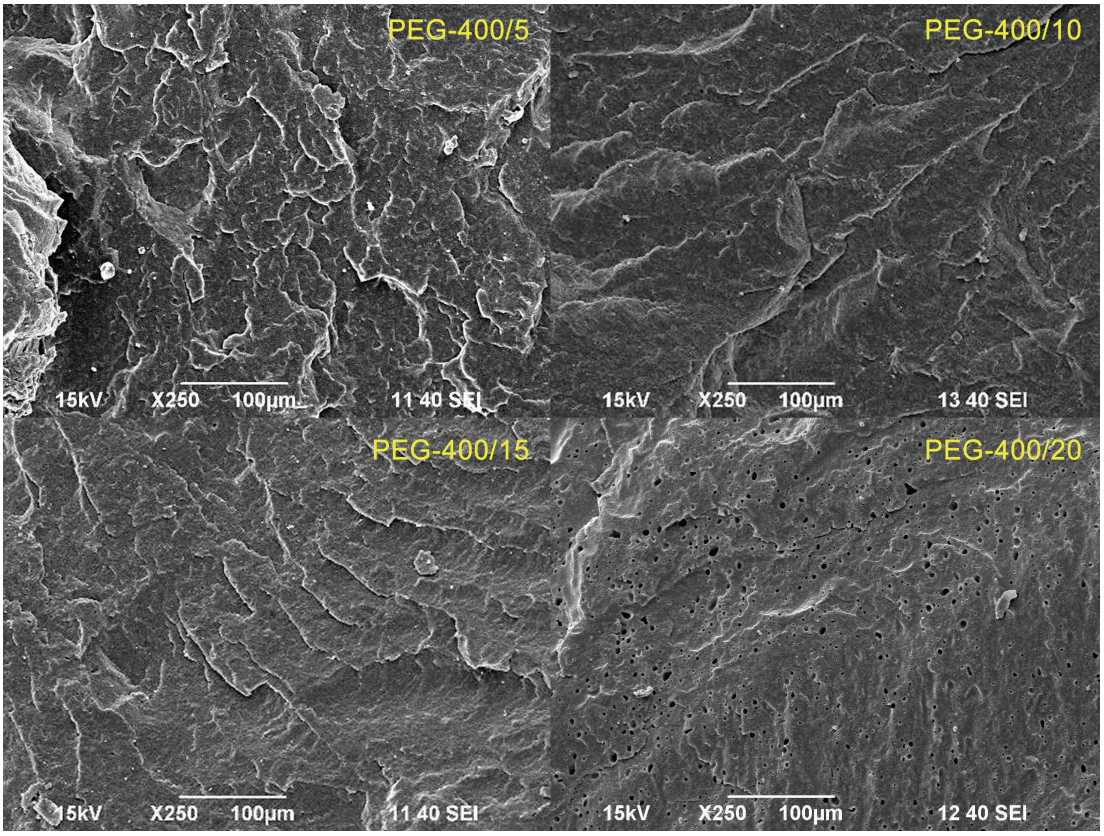

Fig. 2. SEM micrograph of P3HB-based biocomposites containing: 5, 10, 15, and 20 wt. % of PU400 (PEG-400/5, PEG-400/10, PEG-400/15, PEG-400/20, respectively)

the fracture surface. The composite contains 5 wt. % of PU400 (PEG-400/5) showed unevenly distributed rough areas with various stress whitening lines, while the composites 10 and 15 wt. % PU400 (PEG-400/10 and PEG-400/15) exhibited larger and uniformly distributed elongated domains in the composites with no phase separation. However, the SEM micrograph of the samples contained the highest amount of PU400 (i.e., 20 wt. %) displayed a relatively rough surface with flatter and smaller elongated domains with shear deformation and tortuous cracks. It can be confirmed that the addition of 10 and 15 wt. % of PU based on PEG400 in the P3HB matrix led to its reinforcement due to good interfacial compatibility between the components of the tested biocomposites.

The micrographs of P3HB matrix contained different amounts (5, 10, 15, and 20 wt. %) of PU1000 with longer chains of polyol (PEG1000) are presented in Fig. 3. The fracture surfaces appear similar to those previously described. Biocomposite samples containing 5 wt. % PU1000 (PEG-1000/5) exhibited rougher heterogeneously distributed zones, similar to biocompo-

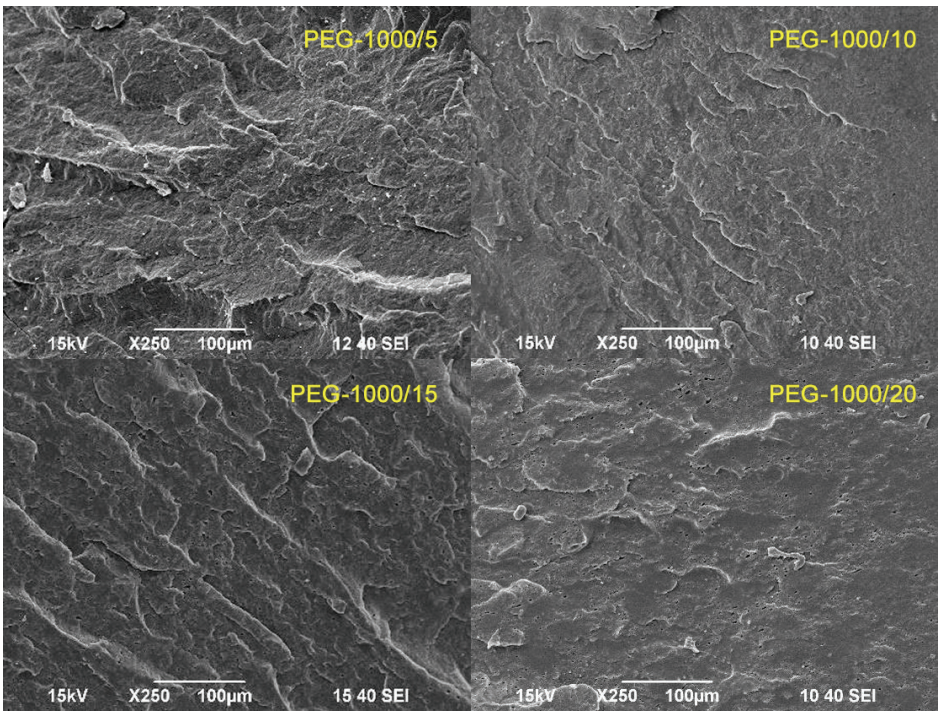

Fig. 3. SEM micrographs of P3HB-based composites containing: 5, 10, 15, and 20 wt. % of PU1000 (PEG-1000/5, PEG-1000/10, PEG-1000/15, PEG-1000/20, respectively)

sites PEG-400/5 (Fig. 2). However, the surfaces of biocomposites 10, 15, and 20 wt. % PU1000 showed rather wave-like and more elongated morphologies which were uniformly distributed. Compared with the unfilled P3HB, the surface of the composites based on PEG1000 is no longer smooth, but exhibits elongated and rough areas.

3.2. Thermal property parameters of the P3HB-based biocomposites

To examine the thermal stability, the resulted biocomposites based on P3HB with 5, 10, 15, and 20 wt. % of PU400 and PU1000 thermogravimetric analysis was carried out. The TGA results are given in Tables 3 and 4.

It was found that the thermal property parameters of the tested biocomposites depend both on the content and the type of polyurethane used. There was a small increase in T_{on}, $T_{50\%}$ and T_{max} by 3–9, 5–7 and 2–3 °C, respectively (Table 3), and even a decrease in those temperatures by 3–24, 3–24, 27–29 °C. Temperature decrease refers to composites PEG-400/20 and PEG-1000/5. In the case of PEG-400/20, it could be caused by the highest plasticizing effect and the highest lowering of crystallinity degree (Table 5). In turn, the composite PEG-1000/5 was not completely homogeneous. Heterogeneity was confirmed by SEM (Fig. 3).

All composites with PU400 have one temperature of maximum decomposition. Addition of 20 wt. %. Of PU400 (PEG-400/20) causes the appearance of the second temperature of the maximum decomposition

Table 3. Interpretation of the TG and DTG curves of P3HB and composites based on P3HB and PU400 and PU1000 recorded at a heating rate of 10 °C·min^{-1} in nitrogen

Composite	T_{on} [°C]	$T_{50\%}$ [°C]	T_{max1} [°C]	T_{max2} [°C]	Δm [%]	Residue at 600°C [%]
P3HB	271	283	287	–	99.38	0.62
PEG-400/5	274	288	290	–	99.30	0.70
PEG-400/10	280	289	290	–	99.38	0.62
PEG-400/15	278	290	289	–	99.51	0.49
PEG-400/20	247	263	258	310	97.98	2.02
PEG-1000/5	248	259	260	377	98.26	1.74
PEG-1000/10	277	288	289	393	99.31	0.69
PEG-1000/15	277	290	289	393	99.29	0.71
PEG-1000/20	268	280	280	395	99.20	0.80

Table 4. Interpretation of the TG and DTG curves of P3HB and composites based on P3HB and PU400 and PU1000 recorded at a heating rate of 5 °C·min^{-1} in nitrogen

Composite	T_{on} [°C]	$T_{50\%}$ [°C]	T_{max1} [°C]	T_{max2} [°C]	Δm [%]	Residue at 600°C [%]
P3HB	236	241	243	–	98.90	1.10
PEG-400/10	266	277	278	–	99.43	0.57
PEG-400/15	268	279	279	–	99.54	0.46
PEG-1000/10	269	279	280	387	99.32	0.68
PEG-1000/15	245	260	261	380	99.06	0.94

rate (T_{max2}), which may indicate the heterogeneity of the system and the exudation of the plasticizer. T_{max2} occurs also in the case of all biocomposites with PU1000.

Biocomposites containing 10 and 15 wt. % of polyurethanes are characterized by the highest thermal stability and for these composites the measurements were repeated at the heating rate of 5 °C min^{-1}. In this case, a significant increase in T_{on}, $T_{50\%}$, and T_{max} was observed 9–33, 19–38, and 18–37 °C, respectively (Table 4). Thermal stability of the PEG-1000/10, PEG-400/10, and PEG-400/15 is comparable and higher than for PEG-1000/15.

The decomposition of all biocomposites materials and the unfilled P3HB occurs in one or two stages in the temperature range of 236–450 °C. The mass loss is usually higher than 99% except for PEG-400/20 and PEG-1000/5 where it is 97.98 and 98.26 wt. %, respectively. Thus, the mass of residues at 600 °C is low and it does not exceed 1 wt. % and in these exceptional cases 2 wt. %.

3.3. DSC analysis of biocomposites

In Figure 4, the dependence of the experimental heat flow rate of P3HB and PU400 composites (5–20 wt. %) on the temperature obtained based on the heating rate

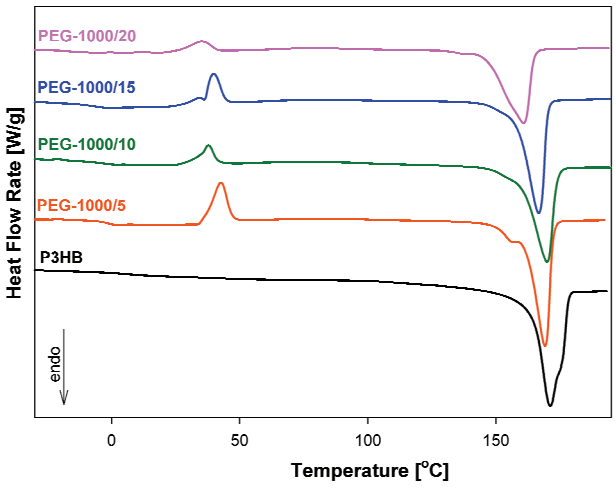

Fig. 4. Comparison of heat flux of P3HB and its biocomposites with PU400 versus temperature

of 10 °C·min^{-1} from the temperature range –40 °C to 195 °C after the previous cooling in the same rate from the temperature range 195 °C to –40 °C.

The qualitative thermal analysis was carried out based on the heat flow rate of the semicrystalline P3HB and its biocomposites. The glass transition and melting were observed during the heating scan for all materials. The cold crystallisation was only recorded for biocomposites between the glass transition and melting region (Fig. 4). All thermal parameters of phase transitions were estimated and listed in Table 5. The change of heat capacity, ΔC_p, and the temperature of glass transition, T_g, were established based on the study of the glass transition region under heating, and the heat of fusion, ΔH_f, and the melting temperature, $T_{m(peak)}$, were also estimated based on the analysis of the melting region. The double peaks were observed for all biocomposites, for example, the smaller endothermic peak of PEG-400/5 occurs at 156.8 °C ($T_{m_1(peak)}$) and is due to the melting of low stability crystals, while the ultimate peak at $T_{m_2(peak)}$ = 169.0 °C corresponds to the melting of the large and more perfect ones. The heat of crystallization, ΔH_c, and the crystallisation temperature, T_c, were analysed under cooling. It can be observed that the modifier (PU400) promotes the crystallisation of composites. The addition of PU400 from 5 to 20 wt. % causes decrease in the temperature of crystallisation, which depends on the amount of additive (Table 5).

The data collected in Fig. 4 relate to the constant value of heating and cooling rate of 10 °C/min. The study with different heating/cooling rates allowed for a different thermal history of biocomposites were also investigated. The results of the changes of heat capacity at T_g versus the heat of fusion obtained based on the different cooling rates were shown graphically in Figs. 5a–d. The P3HB matrix was investigated in the previous paper [21]. Hereby, it should be noted that the changes of heat capacity and other transition parameters were established using the qualitative thermal analysis compared to quantitative thermal analysis described widely in the literature [5], [21]. Most semicrystalline polymeric materials have three phases in the solid state: the crystalline phase (c), the mobile

Table 5. Comparison of the thermal parameters of the P3HB composites with PU400 of representative samples obtained while heating at a rate of 10 °C·min^{-1} after cooling at the same rate

Sample	T_g [°C]	ΔC_p [J·g^{-1}·°C^{-1}]	$T_{m(\text{onset})}$ [°C]	$T_{m1(\text{peak})}$ [°C]	$T_{m2(\text{peak})}$ [°C]	ΔH_f [J·g^{-1}]	T_c [°C]	ΔH_c [J·g^{-1}]
P3HB	7.7	0.1480	159.7	172.2	–	91.9	104.8	88.8
PEG-400/5	0.8	0.090	162.0	156.8	169.0	55.0	41.1	85.2
PEG-400/10	0.7	0.110	161.8	156.6	169.2	48.9	73.3	32.0
PEG-400/15	1.6	0.230	161.0	156.8	169.6	38.0	77.2	26.5
PEG-400/20	–0.6	0.160	160.2	154.3	167.5	32.9	66.6	21.6

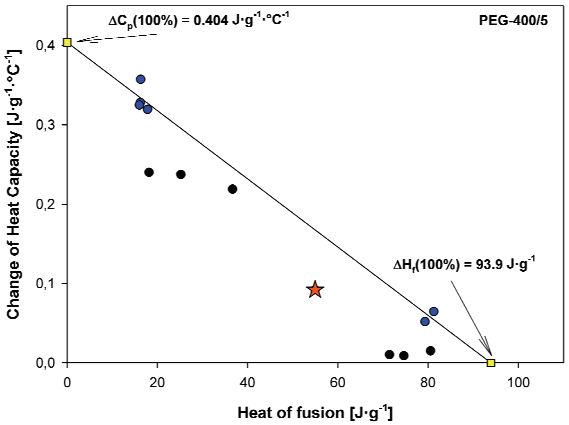

Fig. 5a. The dependence of the heat capacity change at the glass transition temperature on the heat of fusion of the PEG-400/5 composite

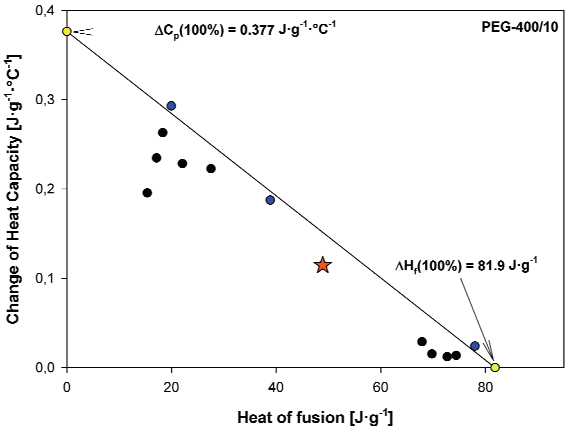

Fig. 5b. The dependence of the heat capacity change at the glass transition temperature on the heat of fusion of the PEG-400/10 composite

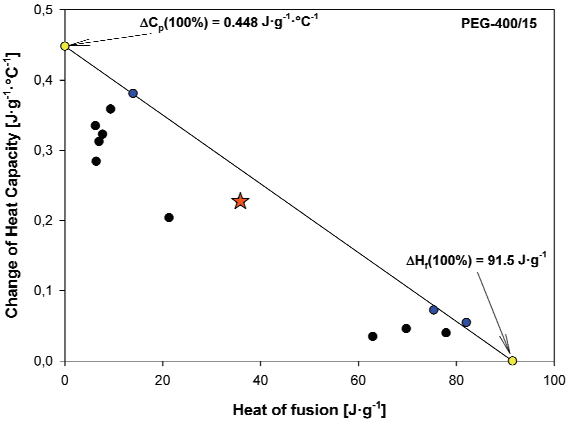

Fig. 5c. The dependence of the heat capacity change at the glass transition temperature on the heat of fusion of the PEG-400/15 composite

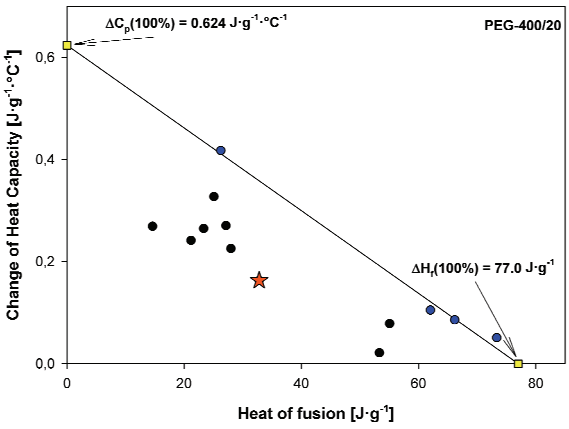

Fig. 5d. The dependence of the heat capacity change at the glass transition temperature on the heat of fusion of the PEG-400/20 composite

amorphous fraction (a), and the rigid amorphous fraction (RAF) [21]. For semicrystalline material which has only two phases (the mobile amorphous phase and the crystalline phase), the plot of the change of heat capacity at T_g versus the heat of fusion gives the linear behavior. The solid straight line was approximated in order to estimate the heat capacity for the fully amorphous sample, ΔC_p (100%), and heat of fusion fully crystalline nanobiocomposites, ΔH_f (100%) by the fitting to experimental data. The ΔC_p (100%) and ΔH_f (100%) of P3HB were obtained from the intersection straight line with the Y and X axes, respectively. The straight line was obtained based on mathematical approximated to the linear equation agree with $y = (-0{,}0043x + 0{,}404)$; $R^2 = 0.9903$. ΔC_p (100%) and ΔH_f (100%) were marked by the yellow squares. The change of heat capacity at T_g for fully amorphous PEG-400/5 was estimated as

0.404 J·g^{-1}·°C^{-1} (68.68 J·mol^{-1}·°C^{-1}) and the heat of fusion for fully crystalline of PEG-400/5 as 93.9 J/g (15.963 kJ/mol). The experimental points which created the solid straight line are characteristic for two phase-model. The points (red star and black circles) outside of the solid line indicate the three-phase model. The red star (Fig. 5a) shows the result of qualitative thermal analysis for PEG-400/5 from the DSC data in Fig. 4. In Figures 6a–d, the dependences of the degree of amorphous phase, W_a, on the degree of crystallinity, W_c, of the P3HB biocomposites with PU400 were shown, respectively. The data from Figures 5a–d were recalculated to W_a and W_c according to $W_a = \Delta C_p/\Delta C_p^{100\%}$ and $W_c = \Delta H_f/\Delta H_f^{100\%}$. The rigid amorphous fraction was estimated as $W_{RAF} = 1 - W_a - W_c$ according to the reference [21]. In Table 6, all estimated equilibrium parameters of P3HB and its biocomposites were listed. Moreover, the analysis of phase content was also added in Table 6. The results refer to the data from qualitative thermal analysis of

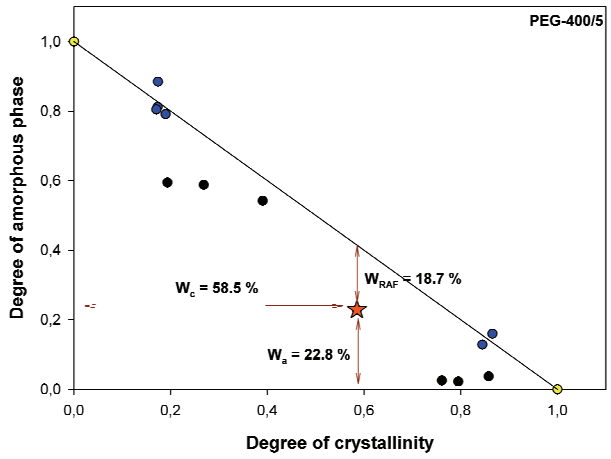

Fig. 6a. The dependence of the amorphous fraction as a function of the degree of crystallinity of the semicrystalline PEG-400/5

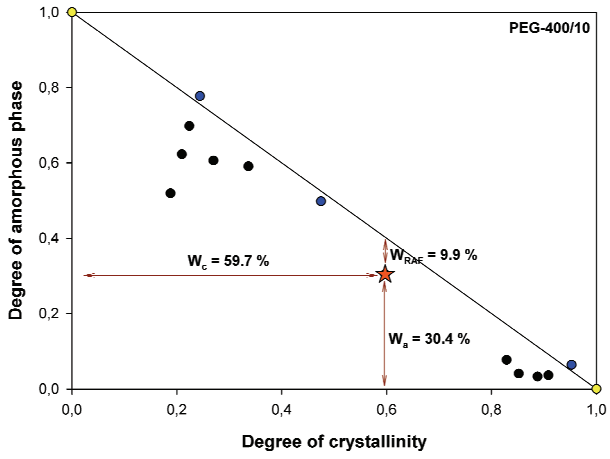

Fig. 6b. The dependence of the amorphous fraction as a function of the degree of crystallinity of the semicrystalline PEG-400/10

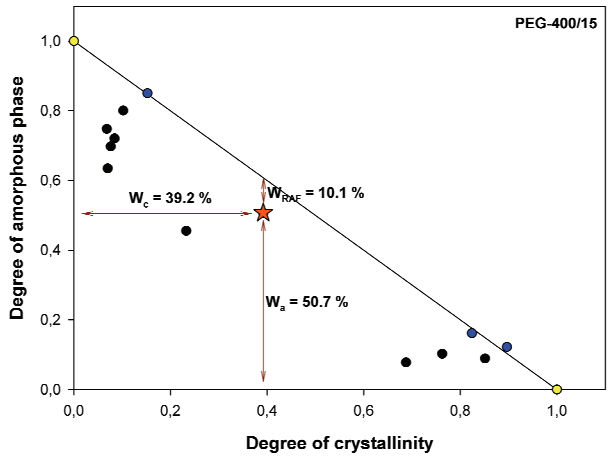

Fig. 6c. The dependence of the amorphous fraction as a function of the degree of crystallinity of the semicrystalline PEG-400/15

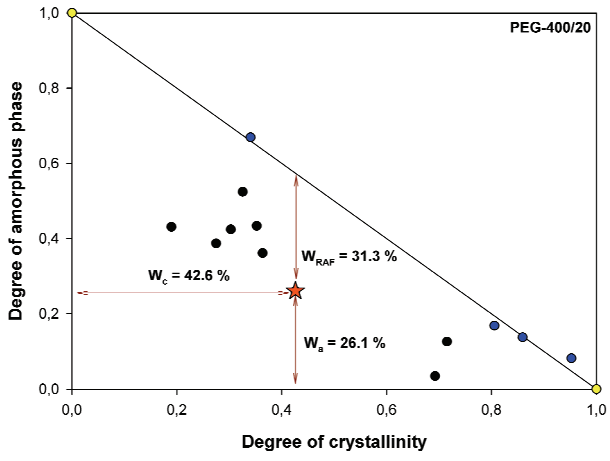

Fig. 6d. The dependence of the amorphous fraction as a function of the degree of crystallinity of the semicrystalline PEG-400/20

Table 6. Comparison of the phase content of P3HB, PEG-400/5, PEG-400/10, PEG-400/15, and PEG-400/20 representative samples obtained by heating at a rate of 10°C·min^{-1} after cooling at the same rate

Sample	W_a [%]	ΔC_p (100%) [J·g^{-1}·°C^{-1}]	W_c [%]	ΔH_f (100%) [J·g^{-1}]	W_{RAF} [%]
P3HB	37.0	0.480	63.0	142.0	0
PEG-400/5	22.8	0.404	58.5	93.9	18.7
PEG-400/10	30.4	0.377	59.7	81.9	9.9
PEG-400/15	50.7	0.448	39.2	91.5	10.1
PEG-400/20	26.1	0.624	42.6	77.0	31.3

P3HB and biocomposites obtained based on the heating rate of 10 °C·min^{-1} from –40 °C to 195 °C and after prior cooling in the same rate from 195 °C to –40 °C (Figs. 6a–d).

In Figure 7, the heat flux rate versus temperature for the P3HB matrix and its biocomposites with PU1000 is shown. The cold crystallization was also observed for all biocomposites in the region between the glass transition and melting.

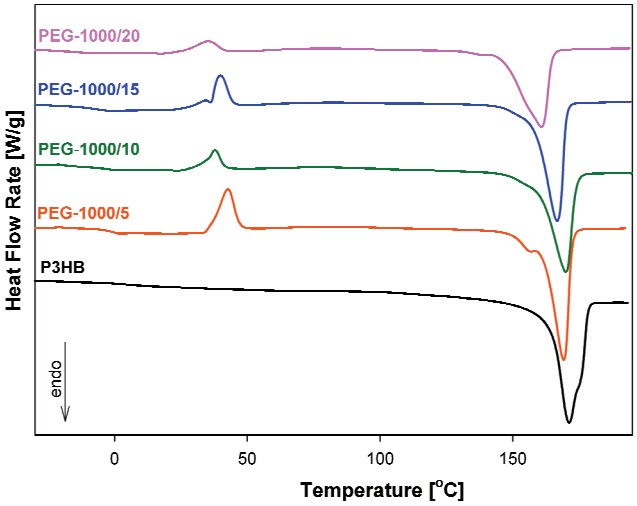

Fig. 7. Comparison of heat flux of composites with PU1000 versus P3HB

The qualitative thermal analysis was performed in a similar manner to the previous one. The results were listed in Table 7. The greatest decrease in the melting temperature ($T_{m(\text{onset})}$) was observed for PEG-1000/20. In the remaining biocomposites, matrix-like values were observed. The formation of a double melting peak was only observed for PEG-1000/5 and the crystallization temperature also decreased for all biocomposites.

In Table 8, all equilibrium parameters of P3HB biocomposites and compared to the P3HB matrix estimated and listed (according to [21]). The analysis of phase content was also carried out and its results were added in Table 8. All analyses were carried out in a similar way as previously for PU400 (Figs. 6a–d).

3.4. Mechanical property parameters

In Figure 8, the tensile strength (TS) and strain at break of P3HB as a function of the amounts of PU400 and PU1000 are shown. TS of all tested compositions decreased with increasing PU content in relation to P3HB. A decrease of approximately 50% and 30% was observed with PU400 and PU1000, respectively. However, it was shown that the strain at break values increased and then decreased with increasing amount of PU400 and PU1000. Maximum improvement of the strain of approximately120% and 15% was exhibited by the compositions based on 5 wt. % PU1000 and 15 wt. % of PU400. The maximum improvement of the strain at break due to the addition of PU1000 and PU400 can be explained by the better ductility and flexibility of polyurethane chains as reported elsewhere [4].

The effect of PU (PU400 and PU1000) content on the impact strength (a) and hardness (b) of P3HB is shown in Fig. 9. Maximum improvement in impact strength (IS) of about 61% over virgin P3HB was exhib-

Table 7. Comparison of the thermal parameters of the P3HB composites with PU1000 of representative samples obtained while heating at a rate of 10 °C·min^{-1} after cooling at the same rate

Sample	T_g [°C]	ΔC_p [J·g^{-1}·°C^{-1}]	$T_{m(\text{onset})}$ [°C]	$T_{m1(\text{peak})}$ [°C]	$T_{m2(\text{peak})}$ [°C]	ΔH_f [J·g^{-1}]	T_c [°C]	ΔH_c [J·g^{-1}]
P3HB	7.7	0.1480	159.7	172.2	–	91.9	104.8	88.8
PEG-1000/5	–1.9	0.277	161.1	156.6	169.1	33.7	77.5	20.7
PEG-1000/10	–3.4	0.063	162.0	–	171.8	39.4	61.4	33.2
PEG-1000/15	–2.9	0.039	160.9	–	168.7	38.9	66.3	59.5
PEG-1000/20	–18.3	0.069	147.6	161.7	139.7	48.7	58.9	33.4

Table 8. Comparison of the phase content of P3HB, PEG-1000/5, PEG-1000/10, PEG-1000/15, and PEG-1000/20 representative samples obtained by heating at a rate of 10 °C·min^{-1} after cooling at the same rate

Sample	W_a [%]	ΔC_p(100%) [J·g^{-1}·°C^{-1}]	W_c [%]	ΔH_f(100%)[J·g^{-1}]	W_{RAF}[%]
P3HB	37.0	0.480	63.0	142.0	0
PEG-1000/5	45.9	0.604	52.5	64.3	1.6
PEG-1000/10	8.3	0.762	52.3	75.4	39.4
PEG-1000/15	4.3	0.788	61.1	63.6	0
PEG-1000/20	14.7	0.463	62.1	78.4	23.2

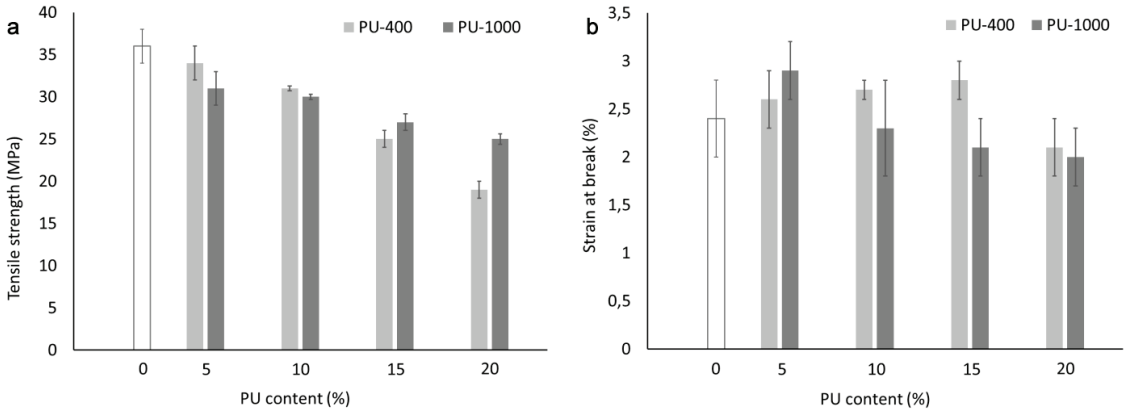

Fig. 8. Effect of PU content on the tensile strength (a) and strain at break (b) of P3HB

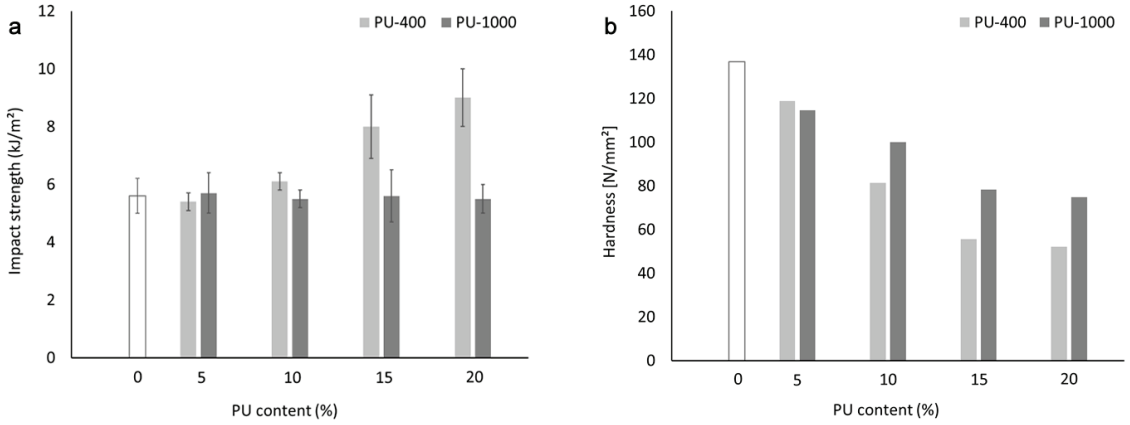

Fig. 9. Effect of PU content on the impact strength (a) and hardness (b) of P3HB

ited by the composition containing 20 wt. % PU400. However, the addition of PU1000 with longer chains did not affect the IS of the tested P3HB compositions.

3.4.1. Statistical analysis

The mechanical property parameters of the obtained biocomposite samples, for which a series of measurements were performed, i.e., tensile strength, strain at break, and impact strength, were subjected to statistical analysis. Its aim was to answer the question of whether the values of the analysed mechanical property parameters of individual composite samples differ from the unfilled P3HB and from one another. Statistical calculations were performed with the Statistica software (version 13). A separate datasheet has been created for each mechanical property parameter. Statistical tests were performed for each of the mechanical property parameters of the obtained samples. Data was verified prior to testing. For this purpose, a normality plot was created for each variable to check for outliers in the data. Such values were removed from the data sheet. Moreover, it was checked whether the variables were normally distributed. Normality was checked using the Shapiro–Wilk test. The significance level $\alpha = 0.05$ was adopted in the tests. The tests of normality showed that the values of tensile strength, strain at break, and impact strength of individual composites have normal distributions. Then the *t*-test (Student's test) was performed. From the calculated values of the *t*-test and the *p*-value it follows that:

a) the tensile strength values are not statistically significant only for PEG-400/5 and PEG-1000/5, i.e., they do not differ from P3HB, while for other composites and P3HB differ significantly;
b) the strain at break value is statistically significant only for PEG-1000/5, i.e., it differs from the unfilled P3HB, while for other composites and P3HB is similar;
c) the impact strength values are statistically significant only for the PEG-400/10, PEG-1000/15, and PEG-400/20 composites, i.e., they differ from P3HB, while for other composites and P3HB are similar.

Then, a one-way analysis of variance (ANOVA) was performed for the examined mechanical property parameters. After checking the differences between

the means of individual variables, *post hoc* tests were performed: Scheffe and Duncan, which allowed: (a) to trace significant differences between the variables and (b) to observe which of the variables form homogeneous groups. The calculated value of the *F*-test (analysis of variance) and the *p*-value show that at least two composites differ in their mechanical property parameters.

The Scheffe test shows that:

a) significant differences in tensile strength exist between the composites PEG-400/15, PEG-400/20, PEG-1000/10, PEG-1000/15, and PEG-1000/20 and other composites and P3HB, moreover P3HB, PEG-400/5, PEG-400/10 and PEG-1000/5 form group I, PEG-400/10, PEG-1000/5, PEG-1000/10 and PEG-1000/15 form group II (overlapping partially with I group), PEG-1000/15, PEG-400/15 and PEG-1000/20 form group III (partially overlapping group II) and PEG-400/20 does not belong to any group;
b) significant differences in strain at break are between PEG-1000/5 and PEG-1000/20, moreover, P3HB, PEG-400/5, PEG-400/10, PEG-400/15, PEG-400/20, PEG-1000/10, PEG-1000/15 and PEG-1000/20 form the first group, P3HB, PEG-400/5, PEG-400/10, PEG-400/15, PEG-400/20, PEG-1000/5, PEG-1000/10 and PEG-1000/15 form group II (overlapping partially with group I);
c) significant differences in impact strength exist between PEG-1000/15 and PEG-400/20 and other composites and P3HB, moreover P3HB, PEG-400/5, PEG-400/10, PEG-1000/5, PEG-1000/10, PEG-1000/15 and PEG-1000/20 form a homogeneous group, and the PEG-400/15 and PEG-400/20 do not belong to any group.

Duncan's test shows that:

a) significant differences in tensile strength do not occur only between P3HB and PEG-400/5, the differences are statistically significant between the other composites and P3HB, moreover P3HB and PEG-400/5 form group I, PEG-400/10, PEG-1000/5 and PEG-1000/10 form group II, PEG-400/15, PEG-1000/15 form group III, PEG-400/15, PEG-1000/20 form group IV (overlapping partially with group III), and PEG-400/20 does not belong to any group;
b) significant differences in strain at break occur between most composites and P3HB, moreover, P3HB, PEG-400/20, PEG-1000/10, PEG-1000/15, and PEG-1000/20 form group I, P3HB, PEG-400/5, PEG-1000/10 and PEG-1000/15 form group II (overlapping group I), and PEG-400/5, PEG-400/10, PEG-400/15 and PEG-1000/5 form group II (partially overlapping group II);
c) significant differences in impact strength occur between PEG-400/5 and PEG-400/10 and between PEG-1000/15 and PEG-400/20 and other composites and P3HB, moreover P3HB, PEG-400/5, 1000/5, PEG-1000/10, PEG-1000/15 and PEG-1000/20 form group I, P3HB, PEG-400/10, PEG-1000/5, PEG--1000/10, PEG-1000/15 and PEG-1000/20 form group II (overlapping group I), and PEG-400/15 and PEG-400/20 do not belong to any group.

Ultimately, statistical tests show that there are statistically significant differences between the biocomposites and P3HB for the three mechanical property parameters tested. Thus, the biocomposites have different mechanical property parameters relative to the unfilled P3HB and among themselves.

3.5. IR spectra analysis

The FTIR spectra of P3HB, PU400, and their composites are presented in Fig. 10. The P3HB spectrum (Fig. 10a) shows a characteristic vibration band of the ester carbonyl groups at 1718 cm^{-1}. Moreover, there are bands of asymmetric and symmetric C–O bonds of the ester, a single one at 1271 and double at 1129 and 1097 cm^{-1}. Two bands of asymmetric and symmetrical vibrations of C–H bonds of methyl and methylene groups are observed at 2990 and 2940 cm^{-1}. Bands above 3000 cm^{-1} are not observed.

In the FTIR spectrum of PU400 (Fig. 10b), a band of valence vibrations of the N–H bond of urethane group is observed in the range of 3600–3100 cm^{-1}. One broad band of valence vibrations of asymmetric and symmetric methylene groups of PU400 is observed in the range of 2800–3000 cm^{-1}. The valence vibration band of the urethane carbonyl groups appears at 1702 cm^{-1}. The bands of asymmetric and symmetric C–O bonds of the urethane groups are visible at 1246 and 1095 cm^{-1}. The last band overlaps the C–O–C valence vibration band in the structural fragment derived from glycol. Bands with a similar position are observed in the IR spectrum of PU1000.

In the FTIR spectrum of P3HB biocomposites with PU400 modifier, the shape of the band above 3000 cm^{-1} was changed. The band intensity above 3000 cm^{-1} was reduced and extended to the range of 3700–3000 cm^{-1}. It was proved that the formation of hydrogen bonds between the urethane groups of the modifier and the ester groups of the polyester. The intensity of this band increased with the increase in the modifier content (Figs. 10c, d). In the 2800–3000 cm^{-1} range, there were 3 bands of asymmetric and symmetric C–H bonds of methyl and methylene groups at 2877, 2933, and

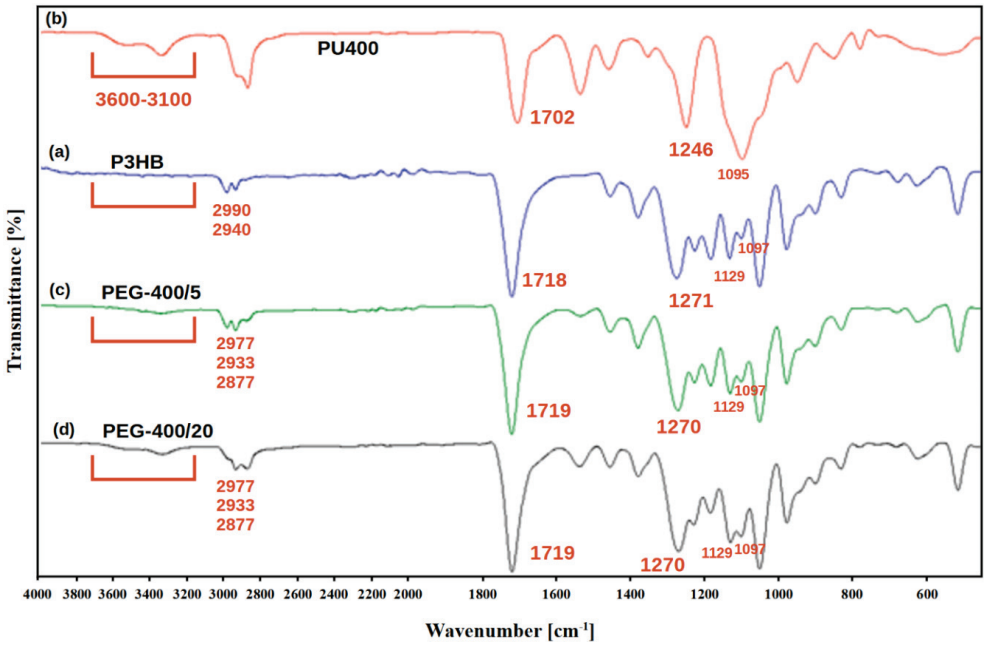

Fig. 10. FT IR spectra of P3HB (a), PU400 (b), PEG-400/5 (c), and PEG-400/20 (d)

2977 cm^{-1}. One combined band of valence vibrations of the C=O groups of ester and urethane was observed at 1719 cm^{-1}. The common band for esters and urethanes for the vibrations of asymmetric C–O bonds appeared at wave numbers lower than 1270 cm^{-1}. The locations of the bands of symmetric vibrations of C–O bonds were unchanged (1129 and 1097 cm^{-1}). The IR spectra of P3HB composites obtained with PU1000 modifier showed similar changes.

4. Discussion

Linear aliphatic polyurethanes based on HDI and polyethylene glycols with a molar mass of 400 g·$mole^{-1}$ (PEG400) and 1000 g·$mole^{-1}$ (PEG1000) – PU400 and PU1000 were used for modification of the P3HB property parameters. The applied polyurethanes were in polymeric form and they were used in the amount of 5, 10, 15, and 20 wt. %.

Reinforcement resulting from good interfacial compatibility between the components of the tested biocomposites is possible due to interactions between the chains of P3HB and PU chains, which was confirmed by FT IR technique. IR spectra of the new biocomposites indicated the formation of hydrogen bonds between the urethane groups of the modifier and the ester groups of the polyester.

The morphology of the resulting biocomposites confirmed that the addition of 5 wt. % and 20 wt. % of PU400 based on PEG400 and 5 wt. % of PU1000 based on PEG1000 (PEG-400/5 and PEG-400/20 and PEG-1000/5) in the P3HB matrix does not lead to homogeneity of components. In general, deformed and rough morphologies are used to explain the increase in fracture toughness of polymers, while a flat and glassy surface is typical of brittle materials with low impact strength and small strain at break. Elongated domains with roughly wavy areas uniformly distributed over the entire surface of the sample explain the improvement of the tensile and impact strengths of polyester composites containing 10 wt. % and 15 wt. % of PU400 and PU1000. Moreover, the presence of plastic yielding may also contribute to an increase in the mechanical property parameters of P3HB composites. Furthermore, the addition, increasing the length of the polyethylene glycol chain resulted in greater flexibility of the polyester with PU1000 than PU400.

The TG analysis of the tested biocomposites indicated that thermal property parameters depend both on the content and the type of polyurethane used. Biocomposites containing 10 and 15 wt. % of polyurethanes were characterized by the highest thermal stability. The increase in initial degradation temperature by 9 °C (to 33 °C) was observed. The highest increase occured in the case of PEG-1000/10, PEG-400/10, and PEG-400/15. Composites with 15 wt % of PU1000 (PEG-1000/15) showed the lower thermal stability.

The qualitative thermal analysis of P3HB and its biocomposites showed the glass transition and melting for all materials and the cold crystallisation only for biocomposites due to a greater disorder of material structure by the introduction of PU400 and PU1000 in the P3HB.

The presence of many peaks during the melting of the polymers is an indication for the existence of different crystalline forms [21] linked tothe introduction of the amount of PU400 and PU1000. It can be seen that the $T_{m(\text{onset})}$ of all biocomposites were similar to that of the P3HB matrix. Furthermore, the plasticization effects of the composites by decreasing the glass transition temperature of the new materials were also observed.

The used modifier PEG-400 decreases the crystallinity content of biocomposites. Introduction of PEG-1000 to the P3HB matrix causes the decrease of the degree of crystallisation for PEG-1000/5 and PEG-1000/10 about 10%. Application of 15% and 20% of PU in the P3HB matrix caused obtaining the degree of crystallinity in the same level as the unfilled P3HB. The increase of degree of crystallinity was observed for PEG-1000/15 about 32% compared to P3HB. The addition of PU from 5 to 20 wt. % causes decrease in the temperature of crystallisation, which depends on the amount of additive (Tables 5, 7).

It can be concluded that the greatest reduction in the degree of crystallinity was observed for composites PEG-400/15 and PEG-400/20. This is due to the plasticization of P3HB by PU400. The PEG-400/15 and PEG-400/20 biocomposites seem to be the most promising in terms of the thermal property parameters, as well as in terms of predicted mechanical property parameters.

The measured mechanical property parameters of the tested biocomposites depended on the type and content of PU used. TS of all tested compositions decreased with increasing PU content compared to the unfilled P3HB. The highest improvement of the strain at break was exhibited by the composites with 5 wt. % (PEG1000/5) and 15 wt. % of PU400 (PEG-400/15). The improvement of the strain at break due to incorporated PU can be attributed to the presence of elastic and flexible chains of polyethylene glycol contained in polyurethane [4]. The impact strength of biocomposites with PU400 increased with increasing PU400 content. In turn, the addition of longer chains of PU1000 did not affect the impact strength of the tested P3HB biocomposites. The significant decrease of hardness might be attributed to the softening and increase of free volume of the composites due to the introduction of flexible chain polyethylene glycol.

5. Conclusions

New biocomposites were produced using P3HB as a matrix and aliphatic linear polyurethanes as modifier in an amount of 5, 10, 15, and 20 wt. %. Aliphatic polyurethanes were obtained based on 1,6-diisocyanate hexamethylene and polyethylene glycols with molecular masses of 400 and 1000 g·mol^{-1}.

The thermal stability of the biocomposites of P3HB-based is higher than the P3HB matrix. The biocomposites PEG-400/15; PEG-400/10 and PEG-1000/10 have the highest growth in the temperature of degradation compared to the unfilled P3HB. The difference was 31–33 °C. The difference between melting temperature and degradation temperature is about 100 °C for most obtained composites.

The DSC analysis revealed the decrease of the glass transition temperature and the degree of crystallinity of the biocomposites. Especially, PEG-400/15 and PEG-400/10 biocomposites seem to be promised, because the greatest reduction in the degree of crystallinity is observed, which was the main goal of our study.

The tested mechanical property parameters of the new biocomposites indicated the increase of strain at break and impact strength and the decrease of tensile strength and hardness of PU400 modified biocomposites with the growth of PU400 content. The mechanical property parameters of the PU1000 modified biocomposites usually decreased or stayed unaffected related to the unfilled P3HB. The best mechanical property parameters had PEG-400/10 and PEG-400/15.

References

[1] ALSAFADI D., AL.-MASHAQBEH O., MANSOUR A., ALSAAD M., *Optimization of nitrogen source supply for enhanced biosynthesis and quality of poly(3-hydroxybutyrate-co-3-hydroxyvalerate) by extremely halophilic archaeon*, Haloferax mediterranei, Microbiol. Open, 2020, 9.

[2] ASHBY R.D., SOLAIMAN D.K.Y., STRAHAN G.D., *The Use of Azohydromonas lata DSM 1122 to Produce 4-hydroxyvalerate-Containing Polyhydroxyalkanoate Terpolymers, and Unique Polymer Blends from Mixed-Cultures with Burkholderia sacchari DSM 17165*, J. Polym. Environ., 2019, 27, 198–209.

[3] ASHORI A., JONOOBI M., AYRILMIS N., SHAHREKI A., FASHAPOYEH M.A., *Preparation and characterization of polyhydroxybutyrate-co-valerate (PHBV) as green composites using nano reinforcements*, Int. J. Biol. Macromol., 2019, 136, 1119–1124.

[4] ASHRAFI M., GHASEMI A.R., HAMADANIAN M., *Optimization of thermo-mechanical and antibacterial properties of epoxy/polyethylene glycol/MWCNTs nano-composites using response surface methodology and investigation thermal cycling fatigue*, Polym. Test., 2019, 78, 105946.

[5] CZERNIECKA-KUBICKA A., ZIELECKI W., FRĄCZ W., JANUS-KUBIAK M., KUBISZ L., PYDA M., *Vibrational heat capacity of the linear 6,4-polyurethane*, Thermochim. Acta, 2020, 683, 178433.

[6] IBRAHIM M.I., ALSAFADI D., ALAMRY K.A., HUSSEIN M.A., *Properties and Applications of Poly(3-hydroxybutyrate-co-3-hydroxyvalerate) Biocomposites*, J. Polym. Environ., 2020.

[7] ISRANI N., VENKATACHALAM P., GAJARAJ B., VARALAKSHMI K.N., SHIVAKUMAR S., *Whey valorization for sustainable polyhydroxyalkanoate production by Bacillus megaterium: Production, characterization and in vitro biocompatibility evaluation*, J. Environ. Manage., 2020, 255, 109884.

[8] KOLLER M., *Switching from petro-plastics to microbial polyhydroxyalkanoates (PHA): the biotechnological escape route of choice out of the plastic predicament?*, The EuroBiotech. J., 2019, 3, 32–44.

[9] KONTÁROVÁ S., PŘIKRYL R., MELČOVÁ V., MENČÍK P., HORÁLEK M., FIGALLA S., PLAVEC R., FERANC J., SADÍLEK J., POSPÍŠILOVÁ A., *Printability, Mechanical and Thermal Properties of Poly(3-Hydroxybutyrate)-Poly(Lactic Acid)-Plasticizer Blends for Three-Dimensional (3D) Printing*, Materials, 2020, 13, 4736.

[10] MA P., CAI X., LOU X., DONG W., CHEN M., LEMSTRA P.J., *Styrene-assisted melt free-radical grafting of maleic anhydride onto poly(β-hydroxybutyrate)*, Polym. Degrad. Stab., 2014, 100, 93–100.

[11] MORALES-GONZALEZ M., ARÉVALO-ALQUICHIRE S., DIAZ L.E., SANS J.Á., VILARIÑO-FELTRER G., GÓMEZ-TEJEDOR J.A., VALERO M.F., *Hydrolytic stability and biocompatibility on smooth muscle cells of polyethylene glycol–polycaprolactone-based polyurethanes*, J. Mater. Res., 2020, 35, 3276–3285.

[12] MORI K., *Poly-3-hydroxybutyrate-based polymer resin composition*, JP5205825B2, 2013.

[13] MORI K., *Poly-3-hydroxybutyrate-based polymer resin composition*, JP5205838B2, 2013.

[14] MORI K., SUZUKI K.-I., *Poly-3-hydroxybutyrate-based polymer resin composition*, JP527756B2, 2013.

[15] NANNI A., MESSORI M., *Effect of the wine lees wastes as cost-advantage and natural fillers on the thermal and mechanical properties of poly(3-hydroxybutyrate-co-hydroxyhexanoate) (PHBH) and poly(3-hydroxybutyrate-co-hydroxyvalerate) (PHBV)*, J. Appl. Polym. Sci., 2020, 137, 48869.

[16] SÁNCHEZ-SAFONT E.L., ARRILLAGA A., ANAKABE J., GAMEZ-PEREZ J., CABEDO L., *PHBV/TPU/cellulose compounds for compostable injection molded parts with improved thermal and mechanical performance*, J. Appl. Polym. Sci., 2019, 136, 47257.

[17] SOLEYMANI EIL BAKHTIARI S., KARBASI S., TOLOUE E.B., *Modified poly(3-hydroxybutyrate)-based scaffolds in tissue engineering applications: A review*, Int. J. Biol. Macr., 2021, 166, 986–998.

[18] SOSA-HERNÁNDEZ J.E., VILLALBA-RODRÍGUEZ A.M., ROMERO-CASTILLO K.D., ZAVALA-YOE R., BILAL M., RAMIREZ-MENDOZA R.A., PARRA-SALDIVAR R., IQBAL H.M.N., *Poly-3-hydroxybutyrate-based constructs with novel characteristics for drug delivery and tissue engineering applications – A review*, Polym. Eng. Sci., 2020, 60, 1760–1772.

[19] VOLOVA T., KISELEV E., ZHILA N., SHISHATSKAYA E., *Synthesis of Polyhydroxyalkanoates by Hydrogen-Oxidizing Bacteria in a Pilot Production Process*, Biomacromol., 2019, 20, 3261–3270.

[20] VOLOVA T., MENSHIKOVA O., ZHILA N., VASILIEV A., KISELEV E., PETERSON I., SHISHATSKAYA E., THOMAS S., *Biosynthesis and properties of P(3HB- co -3HV- co -3H4MV) produced by using the wild-type strain Cupriavidus eutrophus B-10646: Synthesis of PHAs containing 3H4MV by wild strain Cupriavidus eutrophus B-10646*, J. Chem. Technol. Biotechnol., 2019, 94, 195–203.

[21] WUNDERLICH B., *Thermal analysis of polymeric materials*, Springer, Berlin 2005.

[22] YU Z., YANG Y., ZHANG L., DING Y., CHEN X., XU K., *Study on short glass fiber-reinforced poly(3-hydroxybutyrate-co-4-hydroxybutyrate) composites*, J. Appl. Polym. Sci., 2012, 126, 822–829.

[23] ZAIDI Z., MAWAD D., CROSKY A., *Soil Biodegradation of Unidirectional Polyhydroxybutyrate-Co-Valerate (PHBV) Biocomposites Toughened With Polybutylene-Adipate-Co-Terephthalate (PBAT) and Epoxidized Natural Rubber (ENR)*, Front. Mater., 2019, 6, 275.

[24] ZHILA N., SHISHATSKAYA E., *Properties of PHA bi-, ter-, and quarter-polymers containing 4-hydroxybutyrate monomer units*, Int. J. Biol. Macromol., 2018, 111, 1019–1026.